ECOLOGY LETTERS

Ecology Letters, (2012) doi: 10.1111/ele.12022

IDEA AND PERSPECTIVE

Metabolic approaches to understanding climate change impacts on seasonal host-macroparasite dynamics

Péter K. Molnár,[1]* Susan J. Kutz,[2] Bryanne M. Hoar[2] and Andrew P. Dobson,[1,3]

Abstract

Climate change is expected to alter the dynamics of infectious diseases around the globe. Predictive models remain elusive due to the complexity of host–parasite systems and insufficient data describing how environmental conditions affect various system components. Here, we link host–macroparasite models with the Metabolic Theory of Ecology, providing a mechanistic framework that allows integrating multiple nonlinear environmental effects to estimate parasite fitness under novel conditions. The models allow determining the fundamental thermal niche of a parasite, and thus, whether climate change leads to range contraction or may permit a range expansion. Applying the models to seasonal environments, and using an arctic nematode with an endotherm host for illustration, we show that climate warming can split a continuous spring-to-fall transmission season into two separate transmission seasons with altered timings. Although the models are strategic and most suitable to evaluate broad-scale patterns of climate change impacts, close correspondence between model predictions and empirical data indicates model applicability also at the species level. As the application of Metabolic Theory considerably aids the *a priori* estimation of model parameters, even in data-sparse systems, we suggest that the presented approach could provide a framework for understanding and predicting climatic impacts for many host–parasite systems worldwide.

Keywords

Climate change, expected lifetime reproductive output, fitness, host–parasite systems, metabolic theory of ecology, *Ostertagia gruehneri*, R_0, seasonality, Sharpe–Schoolfield model, van't Hoff–Arrhenius relation.

Ecology Letters (2012)

INTRODUCTION

Global climate change is well advanced, and climate models predict that current warming trends will continue, and probably accelerate, in the near future (IPCC 2007). One aspect of climate change that has received considerable attention is the hypothesis that future environmental conditions will alter parasite transmission dynamics. Most early studies asserted that climate change would likely increase the frequency and severity of disease outbreaks and/or lead to parasite range expansions, due to warming-accelerated parasite development, prolonged transmission seasons and other mechanisms (e.g. Harvell *et al.* 2002). Recent studies, however, argue that this picture is probably oversimplified: warmer temperatures may also increase parasite or vector mortality, and these effects may balance or exceed the impacts of faster development. Similarly, increased habitat suitability in one area may be offset by decreased suitability elsewhere, so that a hypothesised parasite range expansion may in reality turn out as a range shift or range contraction (Kutz *et al.* 2009; Lafferty 2009). The complexity of host–parasite systems and knowledge gaps in both theory and data currently prevent conclusive statements regarding climate change impacts on most parasites (Marcogliese 2001; Hoberg *et al.* 2008; Rohr *et al.* 2011). Central theoretical questions, such as what type of host–parasite systems would be most sensitive to climate change, or at which locations climate change will have the greatest impact, have only begun to be addressed (Rohr *et al.* 2011). Predictive models are needed to reliably estimate risk and proactively define control strategies for parasites of humans and wildlife in a changing environment.

Traditionally, host–parasite models are aimed at determining the basic reproductive number R_0 of a parasite (defined as 'the average number of secondary infections that result from introducing one infected host into a population of susceptible hosts' for microparasites, and as 'the expected lifetime reproductive output of a newborn larva' for macroparasites) as a function of the intrinsic parameters of the host–parasite dynamics (Anderson & May 1991). Such parameters may include, for example, birth and death rates of host and parasite, rates of infection or time delays due to parasite development. Many of these parameters are influenced by climate, often nonlinearly, and sometimes in opposing directions (Mangal *et al.* 2008). Evaluating climate change impacts thus requires information on the mathematical relation between environmental covariates and model parameters (Rogers & Randolph 2006). Sometimes, these relationships can be quantified experimentally and then input into host–parasite models to evaluate whether

[1]*Department of Ecology and Evolutionary Biology, Princeton University, Eno Hall, Princeton, New Jersey, 08544, USA*
[2]*Department of Ecosystem and Public Health, Faculty of Veterinary Medicine, University of Calgary, 3330 Hospital Dr. NW, Calgary, Alberta, T2N 4N1, Canada*
[3]*Santa Fe Institute, Santa Fe, New Mexico, 87501, USA*
**Correspondence: E-mail: pmolnar@princeton.edu*

© 2012 Blackwell Publishing Ltd/CNRS

R_0, or other measures of parasitism such as parasite prevalence and burden, will likely increase or decrease under future conditions (Mangal *et al.* 2008; Lafferty 2009). However, the impracticality of developing species-specific models for all climate change impacts on all parasites of humans and wildlife makes it preferable to also develop strategic models (*sensu* May 1973) that can outline broad patterns of expected impacts. Even in cases where insufficient species-specific data prevent a detailed assessment, such models can provide first qualitative predictions and aid the design of mitigation and control strategies. Furthermore, such models can indicate knowledge gaps to help define research priorities for system-specific tactical models.

One path towards a framework of generalised host–parasite models that can account for climatic impacts may be through the 'Metabolic Theory of Ecology' (Brown *et al.* 2004). This theory states that metabolism scales allometrically with body size and exponentially with temperature, or specifically, $I \propto M^{3/4} e^{-E/kT}$, where I represents metabolic rate, M is body mass, E is the average activation energy of respiration, T is temperature in degrees Kelvin, and k is Boltzmann's constant (Gillooly *et al.* 2001). From this basis, the theory derives similar scaling rules for ecological processes and patterns from the organismal to the ecosystem level. The theory has been successful in predicting physiological (e.g. developmental times), demographic (e.g. birth and death rates) and population parameters (e.g. population growth rate, carrying capacity) across a wide variety of taxa (Brown *et al.* 2004). Metabolic Theory has also been applied to explore potential climate change impacts, for example, on ectotherms (Dillon *et al.* 2010) and plant-herbivore systems (O'Connor *et al.* 2011). Although most predictions of Metabolic Theory have not been validated specifically for parasites (Rohr *et al.* 2011), the theory has been applied to explain patterns of parasite abundance and biomass production (Hechinger *et al.* 2011), as well as rates of pathogenesis (Cable *et al.* 2007). Furthermore, allometric equations akin to those of Metabolic Theory have been used in SIR-models of microparasites to estimate transmission rates, to relate the frequency of epidemic outbreaks to host body size, and to analyse how seasonality may affect epidemics (de Leo & Dobson 1996; Bolzoni *et al.* 2008).

Here, we link traditional host–macroparasite models and the concept of R_0 with Metabolic Theory to provide a mechanistic framework that allows estimating parasite fitness under novel environmental conditions. Our models are strategic inasmuch that they are intended for illuminating and predicting general patterns of climate change impacts on macroparasites, but they can also be refined into species-specific tactical models by inclusion of appropriate biological detail to increase prediction accuracy. Of the two cornerstones of Metabolic Theory, we incorporate the exponential relationships between temperature and parasite development and mortality, which have been documented for various parasite species (e.g. Young *et al.* 1980; Smith *et al.* 1986; Smith 1990). We defer inclusion of the allometric scaling of metabolism with body mass to future work, because it remains unclear whether parasites follow the same scaling 'rules' as free-living species (Hechinger *et al.* 2011; Rohr *et al.* 2011). Instead, where parameter values are needed for illustration, we focus on arctic host–parasite systems, because the Arctic – owing to its low species diversity, a strong climate signal, and limited confounding anthropogenic factors – is a particularly good system for unravelling the ecological and epidemiological impacts of climate change (Kutz *et al.* 2009; Molnár *et al.* 2010). For further simplicity, we develop the models for the example of parasitic nematodes with a direct life cycle and endotherm hosts (May & Anderson 1979), but emphasise that these simplifications do not restrict the generality of the framework, and the models can be extended to other parasite life cycles and other ecosystems.

METHODS

Model development

In parasitic nematodes with a direct life cycle, adult parasites reside within the host and produce transmission stages that pass out of the host into the environment. Free-living individuals then pass through several developmental stages until they reach the infective stage and can be taken up again by the host (Fig. 1). Development time to this infective stage depends on metabolic rate, and thus ambient temperature. Mortality of the free-living stages, irrespective of cause (e.g., senescence, predation, environmental factors), is also taken as temperature-dependent (Pietrock & Marcogliese 2003; Brown *et al.* 2004; O'Connor *et al.* 2006; McCoy & Gillooly 2008). The rate of parasite uptake by hosts may or may not be temperature-dependent, depending on the mechanisms determining host–parasite encounters (see Appendix S1 in Supporting Information), and we discuss both the temperature-independent and temperature-dependent cases. Other life cycle components may in general also be influenced by temperature, but for simplicity and to aid clarity of exposition, we only consider temperature effects on the free-living stages and assume no effects on parasites within hosts. Specifically, we consider the case of an endotherm host and further assume sea-

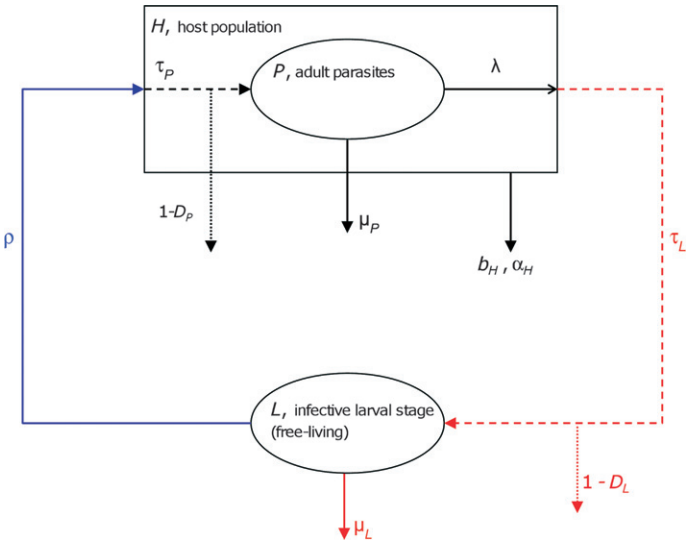

Figure 1 Schematic of a nematode direct life cycle. Boxes represent hosts, adult parasites within hosts, and the free-living larval stage that is infective to hosts. Solid arrows represent the rates that determine losses and gains to each compartment. Dashed arrows indicate the developmental time delays between birth (the moment when newly shed parasites first enter the environment) and infectivity (τ_L), and between uptake and sexual maturity (τ_P) respectively. A proportion of parasites ($1\text{-}D_L$, $1\text{-}D_P$) do not survive these delays (dotted arrows). The delay-length τ_L, the mortality of free-living stages μ_L and the proportion $D_L = \exp(-\mu_L\tau_L)$ are taken to be temperature-dependent (marked red); parasite uptake rate (ρ, blue) may or may not be temperature-dependent (cf. text). All parameters are described in Table 1.

© 2012 Blackwell Publishing Ltd/CNRS

son-independent parasite development to sexual maturity inside the host (i.e. no hypobiosis). Further, we focus on temperature effects only and assume that other environmental covariates are not limiting. Finally, we consider a one-host/one-parasite system with constant host density, ignoring potential interspecific competition for host resources between different parasite species or differing susceptibility to parasites between different host species. Each of these simplifying assumptions can be relaxed to adapt the model to other host–parasite systems.

We follow the classical framework of Anderson & May to represent the host–parasite dynamics within coupled differential equations (Anderson & May 1978; Dobson & Hudson 1992), but modify our models to allow explicitly for a developmental time delay in the free-living stages (Anderson & May 1991):

$$\frac{dL}{dt} = \lambda D_L(T)P(t-\tau_L(T)) - \mu_L(T)L - \rho(T)LH \quad (1a)$$

$$\frac{dP}{dt} = \rho(T)D_P LH(t-\tau_P) - (\mu_P + b_H)P - \alpha_H H\left(\frac{P}{H} + \frac{P^2}{H^2}\frac{k_{NB}+1}{k_{NB}}\right) \quad (1b)$$

Here, L represents the abundance of free-living larvae that are infective to hosts, P is total abundance of adult parasites within hosts, and H is host abundance. Temporal changes in these compartments are determined by the rates of parasite birth (λ), parasite mortality (μ_L, μ_P), host mortality (b_H, α_H) and the rate of parasite uptake by hosts (ρH), as well as the degree of parasite aggregation within the host population, specified by a negative binomial distribution with aggregation parameter k_{NB} (not to be confused with Boltzmann's constant k). All parameters are defined in Table 1. The temperature-dependent parameter $\tau_L(T)$ represents the time delay between the moment when newly shed parasites first enter the environment (hereafter referred to as 'birth') and the moment they reach the infective stage (Fig. 1). Temperature-dependence is also incorporated in the instantaneous mortality of free-living parasites, $\mu_L(T)$, and the composite parameter $D_L(T) = \exp[-\mu_L(T)\tau_L(T)]$, which describes the proportion of parasites that survive from birth to infectivity. For parasite uptake, we initially consider the temperature-independent case, $\rho(T) \equiv \rho_0$, but then also evaluate in Appendix S1 how possible temperature-dependencies in this rate may alter model predictions. All other parameters are temperature-independent as per our assumptions, including the proportion of parasites that survive the prepatent period within the host (of length τ_P) to reach sexual maturity, D_P.

We link the host–parasite dynamics (1) with parasite physiology, and thus temperature, by assuming that mortality (μ_L) and development rate (τ_L^{-1}) of the free-living stages scale with the Boltzmann factor, $e^{-E/kT}$, as predicted by Metabolic Theory (Gillooly *et al.* 2001; Brown *et al.* 2004; McCoy & Gillooly 2008; Munch & Salinas 2009). This relationship, also known as the Van't Hoff–Arrhenius relation, is based on the exponential increase in biochemical reaction rates and metabolic rate with increasing body temperature (Brown *et al.* 2004). Standardising the Boltzmann factor to a reference temperature T_0, development time can be written as (Gillooly *et al.* 2001)

$$\tau_L(T) = \tau_0 e^{\frac{E_\tau}{k}\left(\frac{1}{T}-\frac{1}{T_0}\right)} \quad (2a)$$

and the instantaneous mortality rate as (McCoy & Gillooly 2008)

$$\mu_L(T) = \mu_0 e^{-\frac{E_\mu}{k}\left(\frac{1}{T}-\frac{1}{T_0}\right)} \quad (2b)$$

with the scaling factors τ_0 and μ_0 representing development time and mortality at T_0 respectively.

Although eqn 2 describes temperature dependencies in a broad range of taxa well, it only holds within the 'normal temperature range of activity' (Brown *et al.* 2004). Extrapolation beyond these ranges may yield unrealistic predictions of development or mortality, and consequently of the host–parasite dynamics, at low or high temperatures (cf. Results, Fig. 2). For instance, ectotherms (including parasites) show no detectable development beneath or above certain temperature thresholds (Trudgill *et al.* 2005; Dixon *et al.* 2009). Indeed, the thermal response of most biological traits is unimodal over the full temperature range (Dell *et al.* 2011), and this needs to be incorporated into population models to fully understand climate change impacts (Deutsch *et al.* 2008; Huey *et al.* 2009).

Table 1 Parameter definitions for the host–parasite models represented by eqns 1 and 8

Parameter	Definition	Units
H	Host abundance	—
b_H	Instantaneous host death rate due to causes other than parasitism	time^{-1}
α_H	Instantaneous host death rate where mortality is due to the influence of the parasite	parasite^{-1} time^{-1}
λ	Instantaneous rate of parasite birth *	time^{-1}
μ_L	Instantaneous death rate of the free-living parasite stages	time^{-1}
τ_L	Developmental time from birth to infective stage *	time
D_L	Proportion of parasites that survive from birth to the infective stage [$D_L = \exp(-\mu_L(T)\,\tau_L(T))$] *	—
μ_P	Instantaneous death rate of parasites within the host due to causes other than host death	time^{-1}
τ_P	Length of prepatent period	time
D_P	Proportion of parasites that survive the prepatent period	—
ρ	Instantaneous rate of ingestion of infective larvae by hosts	host^{-1} time^{-1}
k_{NB}	Parameter of the negative binomial distribution that measures the degree of aggregation of adult parasites within the host population	—

*In this context, 'birth' refers to the moment when newly born parasites first enter the environment (e.g. as eggs or first-stage larvae) to become free-living.

© 2012 Blackwell Publishing Ltd/CNRS

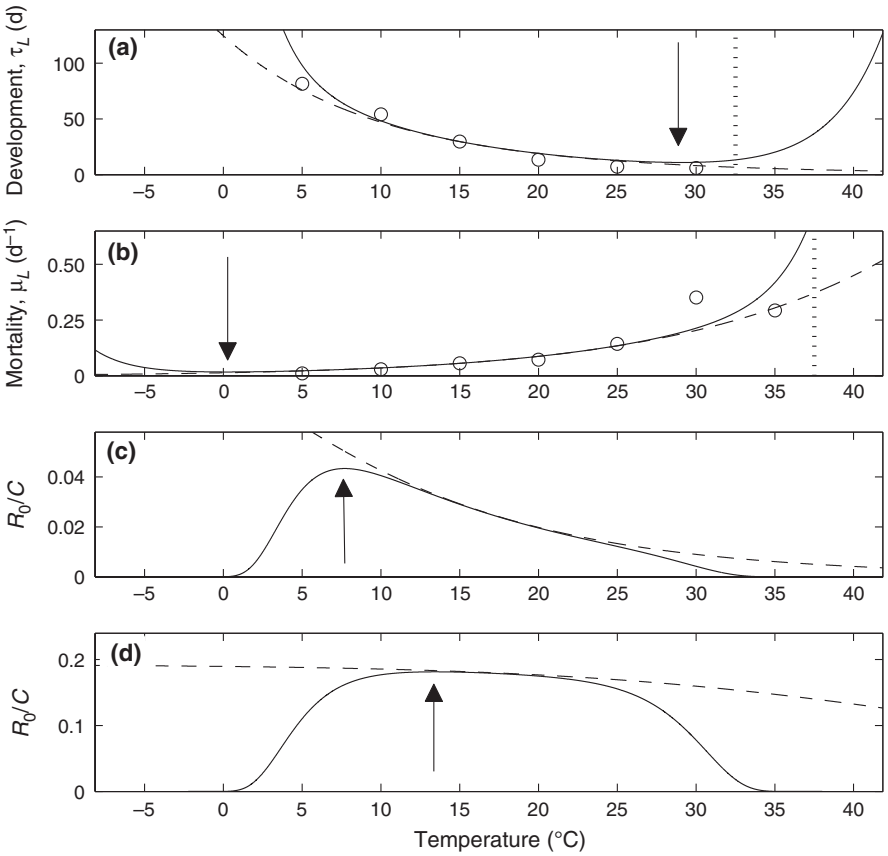

Figure 2 Temperature-dependent predictions, based on eqns 2 (Van't Hoff–Arrhenius; dashed lines) or 3 (Sharpe–Schoolfield development model and our analogous mortality model; solid lines), for (a) time delay between birth and infectivity, (b) instantaneous mortality of free-living parasites, (c)–(d) R_0 (scaled to the constant C, eqn 5) for parasites experiencing (c) low and (d) high uptake respectively (see Table 2 for model parameters). Circles are independently estimated development times and mortality rates of *Ostertagia gruehneri* under laboratory conditions (B. Hoar, unpublished data), indicating excellent fits between model predictions and empirical measurements. Vertical lines indicate temperature thresholds above which (a) *O. gruehneri* cannot develop to infectivity, (b) mortality is immediate. Arrows show optimal temperatures for development, survival, and R_0, when using eqn 3.

Several unimodal models exist to describe development as a function of temperature (e.g. Johnson & Lewin 1946; Sharpe & DeMichele 1977; Schoolfield *et al.* 1981; Régnière *et al.* 2012), of which the Sharpe–Schoolfield model is the most popular. This model provides a natural extension to the Van't Hoff–Arrhenius relation by proposing a reversible inactivation of the rate-controlling enzyme for development at high and low temperatures. The Sharpe–Schoolfield model for development times can be written as

$$\tau_L(T) = \tau_0 e^{\frac{E_\tau}{k}\left(\frac{1}{T}-\frac{1}{T_0}\right)} \cdot \left(1 + e^{\frac{E_\tau^L}{k}\left(\frac{1}{T}-\frac{1}{T_\tau^L}\right)} + e^{\frac{E_\tau^H}{k}\left(-\frac{1}{T}+\frac{1}{T_\tau^H}\right)}\right), \qquad (3a)$$

where E_τ^L and $E_\tau{}^H$ represent the inactivation energies at the lower and upper temperature thresholds, $T_\tau{}^L$ and $T_\tau{}^H$ respectively (Schoolfield *et al.* 1981; Kooijman 2010). Equation 3a results in a concave-up relationship between temperature and development time (Fig. 2a) with curve steepness at the temperature boundaries determined by the inactivation energies. High inactivation energies yield steep increases in development time, and thus sharply defined temperature thresholds. Low inactivation energies allow a more gradual cessation of development with some (slowed) development occurring just below and above $T_\tau{}^L$ and $T_\tau{}^H$ respectively (de Jong & van der Have 2008).

Like development time, mortality frequently deviates substantially from the Van't Hoff–Arrhenius relation at temperature extremes by increasing sharply above and below upper and lower thermal thresholds respectively (e.g. Grenfell *et al.* 1986; Smith 1990; Régnière *et al.* 2012). To capture such threshold behaviours, while simultaneously allowing mortality to follow the Van't Hoff–Arrhenius relation at intermediate temperatures, we consider a mathematically similar extension to eqn 2b as was introduced for development in eqn 3a:

$$\mu_L(T) = \mu_0 e^{-\frac{E_\mu}{k}\left(\frac{1}{T}-\frac{1}{T_0}\right)} \cdot \left(1 + e^{\frac{E_\mu^L}{k}\left(\frac{1}{T}-\frac{1}{T_\mu^L}\right)} + e^{\frac{E_\mu^H}{k}\left(-\frac{1}{T}+\frac{1}{T_\mu^H}\right)}\right) \qquad (3b)$$

Although this equation is partially phenomenological, with the model parameters $E_\mu{}^L$ and $E_\mu{}^H$ lacking a clear enzyme kinetic or other mechanistic derivation, these parameters do have mathematically analogous roles as the inactivation energies of the

© 2012 Blackwell Publishing Ltd/CNRS

Sharpe–Schoolfield development model, determining how abruptly mortality increases at the lower and upper thresholds, T_μ^L and T_μ^H (Fig. 2b).

To evaluate the impact of these temperature-dependencies on total parasite fitness, we consider the basic reproductive number R_0 for system (1),

$$R_0(T) = \frac{\lambda D_P D_L(T)}{\alpha_H + b_H + \mu_P} \cdot \frac{\rho(T)H}{\mu_L(T) + \rho(T)H}, \quad (4)$$

and evaluate this expression as a function of temperature, using either eqns 2 or 3 for development and mortality, and setting $\rho(T)H \equiv \rho_0 H$ (see Appendix S1 for the case where parasite uptake rate $\rho(T)H$ is also temperature-dependent). One key quantity in such analyses is the temperature range where $R_0 \geq 1$, as $R_0 \geq 1$ implies that the parasite could establish under such conditions (Anderson & May 1991). However, whether $R_0 \geq 1$ depends not only on the functions $\tau_L(T)$, $\mu_L(T)$ and $\rho(T)$ but also on the temperature-independent factor $C = \lambda D_P/(\alpha_H + b_H + \mu_P)$. Because we assumed no climate impacts on C, and because the magnitude of C will be species-specific, we keep our analyses general and do not specify this constant. Instead, we evaluate all temperature-induced changes to R_0 relative to C:

$$\frac{R_0(T)}{C} = \frac{D_L(T)\rho(T)H}{\mu_L(T) + \rho(T)H} \quad (5)$$

The effect of seasonality

With the above approach, R_0 is initially estimated as a function of temperature using the simplifying assumption that temperature remains constant year-round. For a more realistic model of climate change impacts, we now relax this assumption to consider seasonal temperature variations. For this, we define

$$T(t) = c_K + d_K \cdot \sin\left((t - t_0) \cdot \frac{2\pi}{365}\right), \quad (6)$$

where $T(t)$ represents temperature in °K on day-of-the-year t, c_K is mean annual temperature, d_K is half the annual temperature range, and t_0 is day-of-the-year when temperature increases to its annual mean (Grenfell *et al.* 1987).

With seasonality added, the temperature-dependent parameters of the free-living stages become variables of time. In particular, the length of the delay between birth and infectivity [previously denoted $\tau_L(T)$] varies with time-of-the-year, and is obtained by integrating over the instantaneous (time-/temperature-dependent) development rates $(\tau_L(T(t)))^{-1}$ experienced by the parasite from birth until development is complete. For this, we define $\tilde{\tau}_L(t)$ as the time delay between birth and infectivity, if infectivity is reached at time t. $\tilde{\tau}_L(t)$can be obtained from

$$1 = \int_{t-\tilde{\tau}_L(t)}^{t} (\tau_L(T(u)))^{-1} du \quad (7)$$

(Grenfell *et al.* 1987; McCauley *et al.* 1996). As the length of the developmental delay is itself a function of time-of-the-year, eqn 1 needs to be re-written:

$$\frac{dL}{dt} = \lambda \tilde{D}_L(t) P(t - \tilde{\tau}_L(t)) \left(1 - \frac{d\tilde{\tau}_L}{dt}\right) - \mu_L(T(t))L - \rho(T(t))LH \quad (8a)$$

$$\frac{dP}{dt} = \rho(T(t - \tau_P)) D_P L H(t - \tau_P) - (\mu_P + b_H)P - \alpha_H H\left(\frac{P}{H} + \frac{P^2}{H^2}\frac{k_{NB} + 1}{k_{NB}}\right) \quad (8b)$$

with $\tilde{\tau}_L(t)$ given by (7), and $\tilde{D}_L(t)$ given by

$$\tilde{D}_L(t) = \exp\left(-\int_{t-\tilde{\tau}_L(t)}^{t} \mu_L(T(u)) du\right), \quad (9)$$

denoting the proportion of parasites that survive from birth at t-$\tilde{\tau}_L(t)$ to infectivity at t (Györi & Eller 1981). If desired, eqns 7–9 can be simplified further algebraically (McCauley *et al.* 1996), but this is unnecessary for our purpose.

To gain a detailed picture of how climate change could affect parasite fitness in a seasonal environment, we use eqns 6–9 to calculate R_0 as a function of parasite birth date for various climate scenarios. For this, we consecutively initialise eqn 8 with a single newly shed egg for all days-of-the-year and calculate expected lifetime reproductive output for each of these birth dates. For comparability with the simplified constant-temperature case, we again scale all estimates of R_0 to $C = \lambda D_P/(\alpha_H + b_H + \mu_P)$.

Model parameterisation

We only parameterise model components that are necessary to calculate $R_0(T)$ according to eqn 5. In this, we set the parameters of the thermal components of Metabolic Theory, that is, the activation and inactivation energies of the Van't Hoff–Arrhenius and Sharpe–Schoolfield models, as predicted by these bodies of theory. For simplicity, we assume equal activation and inactivation energies between development, $\tau_L(T)$, and mortality, $\mu_L(T)$, as predicted by Metabolic Theory (Brown *et al.* 2004). All other parameters (the scaling factors τ_0 and μ_0, and the parameters determining parasite uptake rate, ρ_0 and H), could in theory be scaled allometrically with body size (Brown *et al.* 2004), but we refrain from doing this for the reasons outlined above. Instead, we use the nematode *Ostertagia gruehneri*, which is the most common gastrointestinal parasite of caribou (*Rangifer tarandus*) (Kutz *et al.* 2012), to determine illustrative parameter values. For clarity, we report all temperatures in °C, but note that model input requires transforming these to °K.

Specifically, we set the activation energies $E_\tau = E_\mu = 0.65$ eV, in accordance with empirical measurements of development (Gillooly *et al.* 2001; Brown *et al.* 2004) and mortality (McCoy & Gillooly 2008) across a variety of taxa. The reference temperature T_0 can be chosen arbitrarily for the standard Boltzmann factor (eqn 2), but should be chosen at an intermediate temperature of the thermal development window for the Sharpe–Schoolfield model (eqn 3) because T_0 indicates a temperature where organisms experience little, if any, low or high temperature inactivation (Schoolfield *et al.* 1981). Focusing on arctic parasites, we set $T_0 = 15$ °C. The inactivation thresholds of development were set $T_\tau^L = 2.5$ °C and $T_\tau^H = 32.5$ °C, roughly corresponding to the development thresholds of *O. gruehneri* (B. Hoar, unpublished data). The resulting thermal development window of

© 2012 Blackwell Publishing Ltd/CNRS

Table 2 Parameter definitions and values relating development time and mortality to temperature (eqns 2 and 3). For ease of interpretation, we report all temperature values in degrees Celsius (°C) here; for application in the models, these values are transformed into degrees Kelvin (°K) by adding 273.15 degrees

Parameter	Definition	Value	Units	Sensitivity analyses boundaries	Source
τ_0	Time from birth to infectivity at standardisation temperature T_0	29.6	d	19.7–59.2 d	Based on *O. gruehneri* (B. Hoar, unpublished data; cf. Fig. 2)
μ_0	Instantaneous mortality of free-living parasites at standardisation temperature T_0	0.056	d^{-1}	0.028–0.084 d^{-1}	Based on *O. gruehneri* (B. Hoar, unpublished data; cf. Fig. 2)
E_τ; E_μ	Activation energies regarding parasite development and mortality respectively	0.65	eV	0.2–1.2 eV	(Gillooly *et al.* 2001; Brown *et al.* 2004; Downs *et al.* 2008; McCoy & Gillooly 2008; Irlich *et al.* 2009; Munch & Salinas 2009)
E_τ^L; E_τ^H; E_μ^L; E_μ^H	Low (*L*) and high (*H*) temperature inactivation energies for parasite development (τ) and mortality (μ)	3.25	eV	1.63–4.88 eV	Arbitrary choice based on data from (Schoolfield *et al.* 1981; van der Have 2002; Kooijman 2010), cf. text for details
T_0	Standardisation temperature	15	°C	–	Arbitrary choice at intermediate value of thermal development window (based on *O. gruehneri*, cf. text)
T_τ^L; T_τ^H	Low and high temperature inactivation thresholds for development	2.5; 32.5	°C	–	Based on *O. gruehneri* (B. M. Hoar, unpublished data; cf. Fig. 2)
T_μ^L; T_μ^H	Low and high temperature mortality thresholds	−2.5; 37.5	°C	–	Arbitrary choice, 5 °C below and above T_τ^L and T_τ^H, respectively (cf. text)
k	Boltzmann's constant	8.62×10^{-5}	eV K^{-1}	–	(Gillooly *et al.* 2001)

$T_\tau^H - T_\tau^L = 30$ °C corresponds to the upper end of possible values (Dixon *et al.* 2009), as expected for arctic species (Sunday *et al.* 2011). The viability range $T_\mu^H - T_\mu^L$ is usually larger than the development window (van der Have 2002), so we set the mortality thresholds 5 °C below and above T_τ^L and T_τ^H, respectively, as $T_\mu^L = -2.5$ °C and $T_\mu^H = 37.5$ °C. These thresholds are in agreement with an observed sharp increase in *O. gruehneri* mortality between 35 °C and 40 °C, and also capture the inability of *O. gruehneri* eggs to survive prolonged freezing (B. Hoar, unpublished data; Fig. 2). For the inactivation energies E_τ^L and E_τ^H, the literature provides little guidance, except that generally $E_\tau << E_\tau^L, E_\tau^H$ (Kooijman 2010). We thus arbitrarily chose $E_\tau^L = E_\tau^H = E_\mu^L = E_\mu^H = 5E_\tau = 3.25$ eV, with the multiplier 5 roughly in the range reported by Schoolfield *et al.* (1981), van der Have (2002) and Kooijman (2010). The scaling factors τ_0 and μ_0 (development time and instantaneous mortality at T_0) were set $\tau_0 = 29.6$ d and $\mu_0 = 0.056$ d^{-1}, as observed in *O. gruehneri* (Fig. 2). For the parasite uptake rate $\rho_0 H$, we consider two scenarios as both ρ_0 (parasite ingestion rate by hosts) and H (host abundance) can vary substantially, geographically as well as temporally, both within and between host species (e.g. Stien *et al.* 2002). Specifically, we set $\rho_0 H = 0.01$ d^{-1} and $\rho_0 H = 1$ d^{-1} to represent parasite populations experiencing low and high uptake rates, respectively. All parameter estimates are summarised in Table 2.

Naturally, some or all parameters may differ between species. To illustrate the generality of our results and explore quantitative and qualitative sensitivities of $R_0(T)$, we varied all parameters systematically within broad boundaries. Specifically, we varied E_τ and E_μ between 0.2 eV and 1.2 eV, encompassing the interspecific range of activation energies (Irlich *et al.* 2009; Munch & Salinas 2009). Following Metabolic Theory's prediction of $E_\tau = E_\mu$, we first varied these parameters in conjunction, but then also relaxed the equality constraint to explore consequences for cases where this assumption is violated. All other parameters were varied within +/−50% of their baseline values. For development time, we hereby varied its reciprocal, development rate (τ_L^{-1}), to facilitate sensitivity comparisons with the mortality rate μ_L (Table 2).

For the seasonal model, we defined a baseline climate with $t_0 = 121$ (May 1), mean annual temperature $c_K = 0$ °C and temperature amplitude $d_K = 20$ °C (eqn 6). We then simulated climatic impacts by either increasing the annual temperature mean ($c_K = 0$ °C, 5 °C, 10 °C, 15 °C) or the temperature range ($d_K = 20$ °C, 25 °C, 30 °C, 35 °C). This broad range of scenarios was chosen in an attempt to illustrate the full range of possible climatic impacts across a broad geographical range, encompassing a variety of locations with potentially differing baseline temperatures and climate change scenarios.

RESULTS

Using the predetermined parameter estimates outlined above, and in particular Metabolic Theory's prediction that $E_\tau = E_\mu = 0.65$ eV, both the Van't Hoff–Arrhenius and Sharpe–Schoolfield models capture the observed temperature dependence in *O. gruehneri* development and mortality for most of the temperature range (Fig. 2a,b – note that the models were not fitted to these data, but rather superimposed on them to illustrate the prediction accuracy of the metabolic approach). The Van't Hoff–Arrhenius model, however, fails to predict the lower and upper development thresholds, the high mortality of frozen *O. gruehneri* eggs, or the observed sharp increase in mortality above 35 °C (Fig. 2a,b). Moreover, combining the exponential temperature-dependencies of the Van't Hoff–Arrhenius relation into predictions of $R_0(T)$ leads to monotonically decreasing estimates of $R_0(T)$ within the biologically relevant temperature range (−40 °C to 40 °C) (Fig. 2c,d). This decreasing pattern is observed for a broad range of parameter values (not shown), making the unmodified Van't Hoff–Arrhenius model unsuitable for realistic predictions of $R_0(T)$, especially at the lower and upper temperature extremes.

The Sharpe–Schoolfield development model and our analogous mortality model, in contrast, capture the threshold behaviour of development and mortality, and predict unimodal functions for both these parameters and $R_0(T)$ (Fig. 2). The optimal temperature for development (here, at $T_{opt}^{\tau} = 29.0$ °C; Fig. 2a) usually differs from

© 2012 Blackwell Publishing Ltd/CNRS

the optimal temperature for survival (here, $T_{opt}^{\mu} = 0.3$ °C; Fig. 2b). Consequently, optimal fitness (R_0) is predicted for an intermediate temperature between these two optima, here, at $T_{opt} = 7.8$ °C and $T_{opt} = 13.6$ °C for the low and high parasite uptake scenarios respectively (Fig. 2c,d).

The link between temperature, physiology and fitness allows a first approximation of potential climate change impacts. First, by specifying the temperature range where $R_0(T)$ is expected to exceed one (or equivalently, where $R_0(T)/C \geq 1/C$), the model makes a prediction for the thermal conditions that allow parasite establishment (i.e. the fundamental niche). Second, the magnitude of the predicted $R_0(T)$ can provide a first indicator of the potential severity of parasite infections as a function of temperature. Third, the unimodality of $R_0(T)$ implies temperature ranges where climate warming would increase or decrease parasite fitness (at temperatures below and above T_{opt} respectively). Although the unimodality of $R_0(T)$ is universal, that is, always predicted irrespective of the model parameter values, the location of T_{opt} [i.e. the skewness of $R_0(T)$], the magnitude of $R_0(T)$, and related predictions such as the range where $R_0(T) \geq 1$, can vary with the model parameters.

Parasite uptake rate, for example, influences both shape and magnitude of $R_0(T)$. Whereas low uptake ($\rho_0 H = 0.01$ d^{-1}) yields a right-skewed $R_0(T)$, high uptake ($\rho_0 H = 1$ d^{-1}) masks the influence of physiological temperature-dependencies on $R_0(T)$, leading to a more symmetric $R_0(T)$ with short tails at the temperature extremes (Fig. 2c,d). This is because $\rho_0 H/(\mu_L(T) + \rho_0 H)$ in eqn 5, representing the proportion of infective larvae that enter a host, approaches unity with increasing $\rho_0 H$, while the factor $D_L(T)$ remains approximately constant over a wide temperature range. Hence, we focus on the low uptake scenario from here on.

None of the physiological model parameters act completely independently from each other (de Jong & van der Have 2008). Nevertheless, they mostly affect different characteristics of $R_0(T)$ which can be classified as follows. The baseline development time, τ_0, and mortality rate, μ_0, affect the magnitude of $R_0(T)$ over all temperatures, but not the location of T_{opt} (Figure S1a). For the current parameter set, $R_0(T)$ is hereby more sensitive to changes in mortality than development. The inactivation energies (E_τ^L, E_μ^L, E_τ^H, E_μ^H) in contrast, only affect $R_0(T)$ at the lower and upper ends of the temperature niche (Figure S1b,c). Model predictions are comparatively insensitive to these parameters, particularly at high temperatures. Further, $R_0(T)$ is qualitatively insensitive to temperature thresholds (T_τ^L, T_μ^L, T_τ^H, T_μ^H) which only shift $R_0(T)$ along the temperature axis.

The key parameters that affect both the qualitative shape and magnitude of $R_0(T)$ are the activation energies E_τ and E_μ, which specify the slopes of $\tau_L(T)$ and $\mu_L(T)$ respectively (Fig. 3a,b). If varied in conjunction, they affect magnitude and kurtosis of $R_0(T)$, but maintain the right-skewed shape (Fig. 3e). However, increasing E_τ from 0.2 eV to 1.2 eV, while fixing $E_\mu = 0.65$ eV, changes $R_0(T)$ from right-skewed to left-skewed for the current parameter set. This change in skewness is due to the contrasting decrease and increase of development time at high and low temperatures, respectively, caused by the increasing slope of $\tau_L(T)$. Increasing E_μ from 0.2 eV to 1.2 eV, while fixing $E_\tau = 0.65$ eV, acts in the opposite direction, changing $R_0(T)$ from left-skewed to right-skewed, for analogous reasons (Fig. 3). These structural sensitivities may have far-reaching implications, as the impacts of climate change on a parasite population depend fundamentally on the skewness of $R_0(T)$ as discussed below.

The effect of seasonality

One key limitation of the above analyses is the simplifying assumption that temperature remains constant year-round. In a seasonal environment, however, not all parasites are born equal, as their expected lifetime reproductive output, R_0, depends on the climate that the free-living stages experience while developing, and hence on parasite birth date. With the chosen parameters and a baseline environment with mean annual temperature $c_K = 0$ °C and temperature amplitude $d_K = 20$ °C (Fig. 4, black lines), development rate peaks around early-August, and is zero before early-May and after mid-October (Fig. 4b). Mortality, in contrast, is lowest during the intermediate temperatures of spring and fall (Fig. 4c), reflecting the different optimality conditions of development and survival (Fig. 2a, b). For most of the year, these contrasting effects approximately balance out for the developmental stages, resulting in ~19% of parasites surviving from birth to infectivity between mid-May and early-September (Fig. 4d). Nevertheless, the synthesised predictions for R_0 still show a slight mid-summer trough due to the increased, high-temperature-induced mortality that parasites experience between having reached infectivity and finding a host (Fig. 4e). R_0 is zero for parasites born before early-April and after mid-September (Fig. 4e), reflecting the assumption of high mortality at low temperatures (Fig. 4c, cf. also Fig. 2b).

In warmer conditions, the summer trough in R_0 becomes more pronounced due to the expected increase in summer mortality (Fig. 4a–e, blue and green lines). In more extreme conditions (Fig. 4a–e, red lines), summer development may also slow down due to enzyme inactivation or other processes that slow biochemical reactions (Fig. 4b) and summer mortality may further increase to a point (Fig. 4c), where the majority of summer-born parasites cannot survive to infectivity (Fig. 4d). Due to this, the model suggests that climate warming may split a previously continuous spring-to-fall transmission pulse into two separate transmission pulses, a smaller one in spring, and a larger but shorter one in fall (Fig. 4e). The fall peak is larger, because for spring-born larvae the rising spring temperatures result in progressively increasing mortality rates for the period between having reached infectivity and finding a host, whereas for fall-born larvae the opposite is true (Fig. 4c). As this mortality source becomes less important with increasing parasite uptake rates (cf. $\rho_0 H$ in eqn 5), the magnitude of the spring and fall peaks is approximately equal in a high uptake scenario (Figure S2). The timing of the transmission pulses is also expected to shift with climate warming, towards earlier in spring and later in fall (Fig. 4e), potentially even wrapping around to allow winter transmission (Figs. 4e, S2a, red lines). These phenological changes are observed because milder spring and fall temperatures would allow parasite development progressively earlier and later in spring and fall, respectively (Fig. 4b), while simultaneously reducing parasite mortality in these seasons (Fig. 4c,d). Whether the opposing effects of a decreasing R_0 in summer and increasing R_0 in spring and fall lead to an overall increase or decrease in R_0 can be evaluated by averaging $R_0(t)$ over the entire year (Heesterbeek & Roberts 1995). However, such analyses are beyond the scope of this study as the evaluation also depends on (species-specific) parameters other than those quantified here (i.e. those incorporated in C).

The above results were based on climate scenarios where mean annual temperature (c_K) was varied but the annual temperature

© 2012 Blackwell Publishing Ltd/CNRS

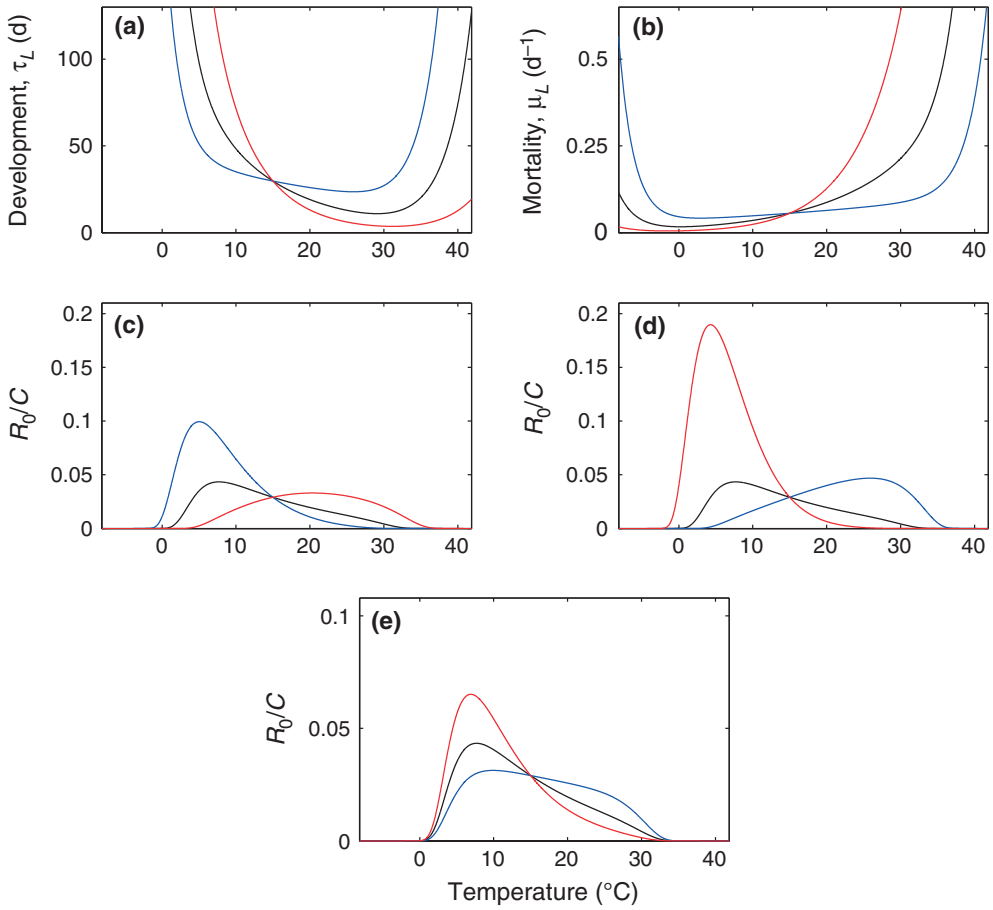

Figure 3 Sensitivity of development time ($\tau_L(T)$), mortality rate ($\mu_L(T)$) and $R_0(T)$, to the activation energies E_τ and E_μ. Effects are shown for decreasing (blue lines) or increasing (red lines) E_τ and E_μ from 0.65 eV (black lines) to 0.2 eV and 1.2 eV respectively. (a)–(d) Left column shows the effects of varying E_τ with E_μ = 0.65 eV fixed; right column shows the reverse case. The first row shows the effects on $\tau_L(T)$ and $\mu_L(T)$; the second row shows the resultant changes in $R_0(T)$ (note the different sensitivities to development and mortality). (e) Sensitivity of $R_0(T)$ when varying E_τ and E_μ simultaneously under the constraint $E_\tau = E_\mu$. Results are based on the Sharpe–Schoolfield development model, our analogous mortality model, and the low uptake scenario.

range, specified by d_K in eqn 6, was held constant. However, temperature range will vary between locations, particularly across latitudinal gradients, and may also be affected by climate change. We therefore illustrate the effect of temperature range on model outcomes in a second set of climatic simulations, where we varied range but kept annual mean temperature constant (Fig. 4f). Here, an increasing range results in increasing summer temperatures as before (Fig. 4f), yielding similar patterns of summer development, summer mortality and summer R_0 as described above (Fig. 4g–j). In contrast to the previous case where increasing mean temperatures resulted in earlier spring and later fall transmission pulses, increasing temperature variability now shifts the season that allows a positive R_0 towards later in the year, in both spring and fall (Fig. 4j). In spring, these patterns arise because early-spring temperatures are highest under the scenario with the lowest temperature range (Fig. 4f, black line; note the 'temperature switch-over' between scenarios at t_0 = 121) resulting in the lowest early-spring mortality for this case (Fig. 4h). In fall, the latest transmission season is observed with the highest temperature variability because the warmer fall temperatures allow for development to be sufficiently fast to compensate for increases in mortality (Fig. 4g–i). Changes in transmission season timing due to increasing temperature range are small compared with the case with increasing mean temperatures, because fall temperatures drop faster with increasing temperature range, resulting in a faster increase in fall mortality and faster decrease in development rate (compare Figs. 4b,c with 4g,h). These contrasting patterns illustrate the necessity to consider changes both in mean temperature and in temperature range and variability in climate-linked host–parasite models.

All of the above conclusions hold when temperature-dependence is also incorporated in parasite uptake rate, $\rho(T)H$. Even though a highly temperature-sensitive $\rho(T)H$ may affect the skewness of $R_0(T)$ in the simplified case of no seasonality (Figure S3), model predictions regarding climate change impacts (in particular, concerning phenological changes and the appearance of a summer fitness trough) are qualitatively and quantitatively similar between the temperature-independent and temperature-dependent uptake cases when seasonality is considered (Figures S4, S5). The only notable difference between these two cases concerns the magnitude of the spring and fall peaks, which are approximately equal when uptake rate is described by the Van't Hoff–Arrhenius relation or a temperature-dependent unimodal model (cf. Appendix S1 for details).

© 2012 Blackwell Publishing Ltd/CNRS

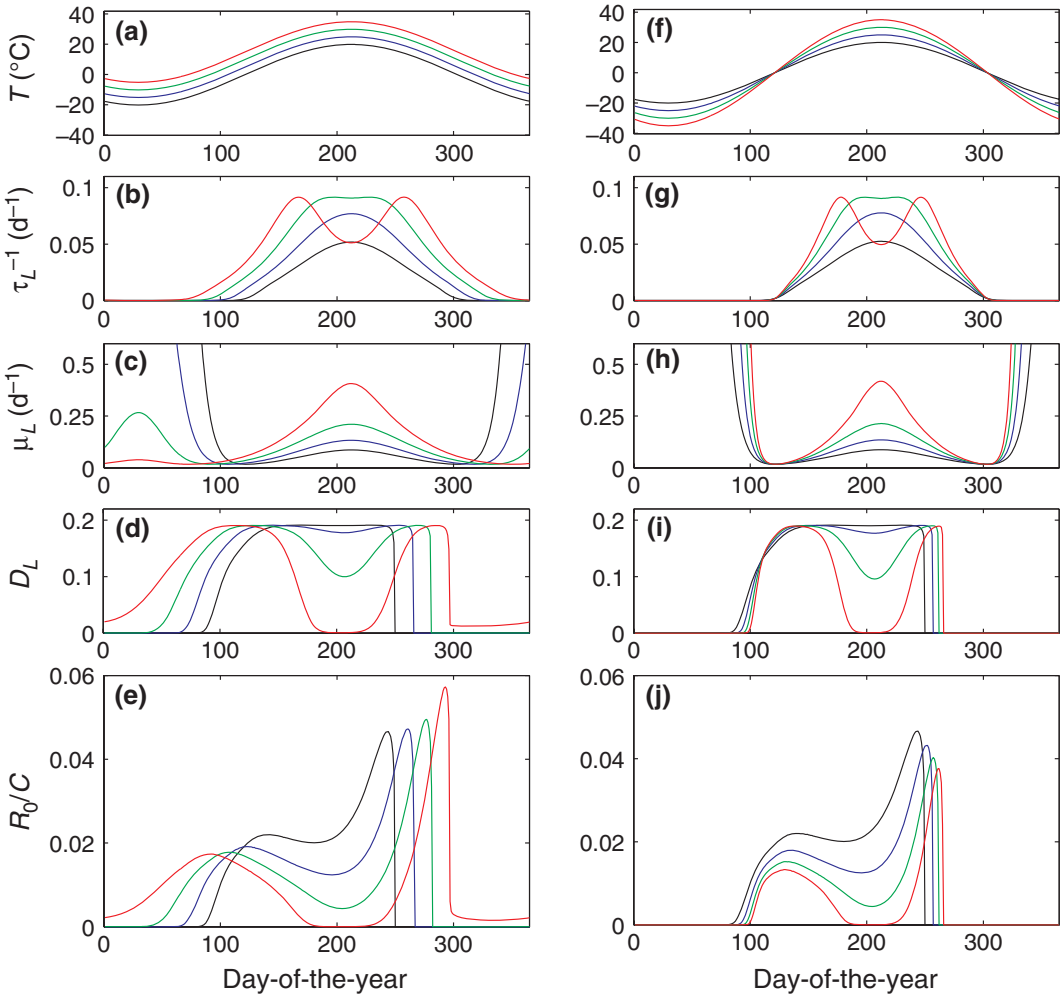

Figure 4 Model predictions (eqns 3, 6–9) for climate change impacts on seasonal parasite development, mortality, and R_0. (a) Four seasonal climate scenarios with annual temperature amplitudes d_K = 20 °C and mean temperatures c_K = 0 °C (black), 5 °C (blue), 10 °C (green) and 15 °C (red). (b) Day-of-the-year-specific instantaneous development rates, τ_L^{-1}, for the parasite stages between birth and infectivity. (c) Day-of-the-year-specific instantaneous mortality rates, μ_L, for free-living parasites. (d) Resultant probabilities to survive from birth to infectivity, D_L, as a function of parasite birth date. (e) R_0, scaled to $C = \lambda D_P/(\alpha_H + b_H + \mu_P)$, as a function of parasite birth date for the low uptake scenario. (f)–(j) are as (a)–(e) but based on climate scenarios with mean temperatures c_K = 0 °C and temperature amplitudes d_K = 20° C (black), 25 °C (blue), 30 °C (green), and 35 °C (red).

DISCUSSION

Predicting the impacts of climate change on the dynamics of host–parasite systems is challenging due to the intrinsic complexity of multi-species interactions and the numerous ways in which the environment can influence such dynamics (Lafferty 2009; Rohr *et al.* 2011). Here, we have linked parasite physiology with parasite population dynamics, an approach that allows integrating multiple nonlinear temperature-dependencies within a single measure of fitness (R_0) to evaluate the net effect of positive and negative climate change impacts on different aspects of parasite life history. Our model is an advance over traditional approaches, such as degree-day models (Kutz *et al.* 2005; Trudgill *et al.* 2005) or models using Q_{10} (Poulin 2006), which can only quantify temperature-dependent changes to a single life history component, such as development, mortality or fecundity, one at a time. Furthermore, our analyses have shown that it is necessary to account for the frequently observed unimodal shape of parasite development and mortality to realistically model climate change impacts across the full range of possible baseline temperatures. Consequently, we have chosen extensions of the standard Van't Hoff–Arrhenius relation to include upper and lower thermal thresholds for changes in development and mortality, and the unimodal shape of these functions carries over to $R_0(T)$. Ultimately, our model embraces the idea that climate change can have both positive and negative impacts on parasite fitness (Lafferty 2009), and explicitly derives this result from first principles.

In its current form, the framework focuses on the physiological consequences of parasite exposure to different temperatures. As such, it is suitable for determining the fundamental thermal niche of a parasite under both current and novel environmental conditions. An estimate for the geographical expanse of this niche can be obtained by determining where temperatures are such that $R_0 \geq 1$ (Rogers & Randolph 2006). For this, depending on the desired resolution, one could use the simplified model without seasonality (eqn 5) as a first approximation (but see Savage 2004 for limitations of this approximation), or integrate over the season-dependent esti-

© 2012 Blackwell Publishing Ltd/CNRS

mates of R_0 that emerge from the sinusoidal temperature model (6) (Heesterbeek & Roberts 1995; Caswell 2011). Incorporating daily temperature fluctuations and stochasticity into eqn 6 – and assessing the consequences for R_0 – may hereby be another key step in further increasing prediction accuracy, because larvae often cannot survive extremely high temperatures even for short periods (Fig. 2b), and may thus be affected substantially by the predicted increase in the frequency of extreme temperature events (IPCC 2007).

Geographical changes to the fundamental niche under future conditions could be obtained by linking local climate predictions with R_0. For illustration, consider interpreting the unimodal $R_0(T)$ of the simplified model (Fig. 2c) geographically, with the left and right ends of the *x*-axis corresponding to the high-latitude (low temperature) and low-latitude (high temperature) edges of a hypothetical parasite range. Uniform warming across this range would result in decreasing parasite fitness in the southern parts of the range, and increasing fitness in the northern parts (with the two impact regions roughly separated by T_{opt}). The shape of $R_0(T)$ (together with predicted climate maps) hereby determines whether the parasite would experience a range contraction, a range shift, or whether it could theoretically even expand its range based on its physiological constraints. With a right-skewed $R_0(T)$, a uniformly warmer climate would result in decreasing parasite fitness over most of its range, implying a likely range contraction. A left-skewed $R_0(T)$ would indicate that climate warming would likely increase the parasite's potential to expand its range, with range contractions at the southern range edge possibly outweighed by range expansions at the northern edge.

One key limitation of the models in their current form is that they do not include various abiotic and biotic factors, such as dispersal barriers, competition with other parasite species, and climate or land use impacts on host ranges. Each of these factors may limit or facilitate parasite range expansions. Consequently, our models allow predicting negative climate change impacts on parasites, such as where the habitat becomes unsuitable to support a given species, but they cannot predict whether physiologically permissible range expansions will actually occur (Dobson & Carper 1992; Lafferty 2009). Similarly, considering the effects of seasonality, and thus the fundamental *temporal* niche of a parasite, it is likely that predictions concerning seasonal reductions in R_0 would be associated with less uncertainty than predictions concerning expansions of the season where R_0 is positive (as the latter also requires host availability at potentially unusual times of the year). In other words, the models can predict changes to a parasite's (geographical or temporal) fundamental niche, but not changes to its realised niche (Lafferty 2009). However, Metabolic Theory and related theories, such as Dynamic Energy Budget Theory, have been successful in quantifying patterns and processes across all levels of biological organisation (Nisbet *et al.* 2000; Brown *et al.* 2004; Kearney *et al.* 2010). Moreover, the ideas of Metabolic Theory have also been applied to explain dynamical interactions, for example in herbivore-plant systems (O'Connor *et al.* 2011), predator–prey systems (Vasseur & McCann 2005) and carbon cycling (Allen *et al.* 2005). Thus, it may be possible to extend our framework to include population-, community- and ecosystem-level processes within parasite models of different complexity to also aid the prediction of realised niches.

Another advantage of parameterising parasite models using Metabolic Theory is that this allows first approximate estimates of the temperature-dependence and magnitude of all model parameters, and thus the likely qualitative shape of $R_0(T)$. Given the practical impossibility of determining climate change impacts on all existing and emerging parasites separately, this property could be used for broad-scale risk analyses, and would be particularly useful in species where little to no data exist. Using Metabolic Theory as a predictive tool across parasite species necessitates confronting, validating and possibly modifying the theory with extensive parasite data first, as has been done for free-living species (Brown *et al.* 2004; Dell *et al.* 2011). To determine climate change impacts on $R_0(T)$, it is, for example, key to accurately quantify the activation energies E_τ and E_μ *a priori* (Fig. 3). Estimating these activation energies can be accomplished in various ways, but might be easiest by fitting eqns 2 or 3 to temperature-dependent development/mortality data, obtained from cohorts of larvae reared at a range of different temperatures (e.g. see Schoolfield *et al.* (1981), Smith *et al.* (1986) and Smith (1990) for computationally simple nonlinear regression approaches, and Régnière *et al.* (2012) for more precise maximum-likelihood methods). Although Metabolic Theory predicts that E_τ and E_μ would lie between 0.6 eV and 0.7 eV in most cases, a broader range for these parameters, approximately spanning 0.2 eV to 1.2 eV, has also been suggested (Downs *et al.* 2008; Irlich *et al.* 2009). Within this range, $R_0(T)$ may change from right-skewed to left-skewed (Fig. 3), a switch with fundamental implications as outlined above.

To date, it remains unclear whether parasites follow the same metabolic 'rules' as free-living species (Rohr *et al.* 2011), although it seems probable that this would hold at least for free-living stages. In *O. gruehneri*, the predicted activation energies $E_\tau = E_\mu = 0.65$ eV explain the temperature-dependence of development and mortality extremely well (Fig. 2). Moreover, the resulting predictions of a summer trough in development, survival and R_0 (Fig. 4) qualitatively correspond with field and experimental warming data of this species (Hoar *et al.* 2012). Although these results are encouraging, it remains difficult to determine whether similar activation energies also apply to other species, as few standardised descriptions of parasite development and mortality exist (e.g. some studies define development time as 'time until appearance of first infective larva' while others report the 'time when 50% of eggs have developed to infectivity'; moreover, mortality and development are seldom separated out in such studies; e.g. Young *et al.* 1980; Kutz *et al.* 2001). Nevertheless, preliminary analyses of development ($n = 6$) and mortality ($n = 13$) data on the free-living stages of parasitic nematodes support the hypothesis that the thermal component of Metabolic Theory holds as in free-living species (Fig. 5). Although these analyses are not intended to be exhaustive, and may also be affected by protocol differences between source studies, they are encouraging. The median and mean activation energies for both development (median: 0.67 eV, mean: 0.62 eV) and mortality (median: 0.67 eV, mean: 0.70 eV) closely correspond to the predicted 0.65 eV. Further, the majority of estimates fall in or near the narrow 0.6–0.7 eV range, and all estimates are well within the wider expected 0.2–1.2 eV range (Fig. 5). Regarding the second component of Metabolic Theory – the allometric scaling of metabolic rates with body mass – even less information is available for parasites. Indeed, the standard theory may have to be modified to account for additional covariates, processes and species interactions, such as humidity, host immune reactions or trophic level (Hechinger *et al.* 2011). Finally, it remains unclear whether variation in other model components, such as threshold temperatures or inactivation energies, could also be described using Metabolic Theory. These questions delineate fruitful lines for further investigation.

© 2012 Blackwell Publishing Ltd/CNRS

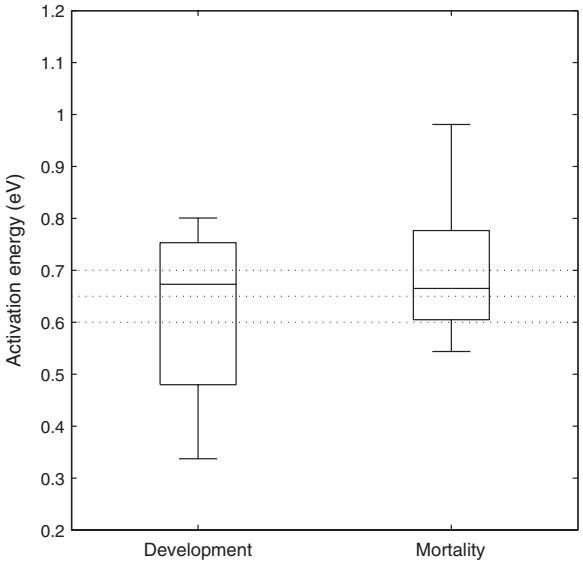

Figure 5 Activation energies for development to infectivity (E_τ) and mortality of free-living infective larvae (E_μ), obtained by fitting eqns 2a and 2b to temperature-dependent development and mortality data of parasitic nematodes (see Table S1 for data sources). The horizontal lines show the mean activation energies predicted by Metabolic Theory, $E_\tau = E_\mu = 0.65$ eV, and the 0.6–0.7 eV range (cf. text).

Although we expect Metabolic Theory to be particularly useful for broad-scale analyses, the simultaneous development of tactical models (species-specific models with much biological detail; e.g. Grenfell *et al.* 1987; Mangal *et al.* 2008) will be key for furthering theory and for improving prediction accuracy in selected systems. For this, the presented approach could still serve as a framework, and offers great flexibility for assessing a wide range of temperature responses both within and between species, as the models allow accounting for any combination of activation energies, inactivation energies and temperature thresholds in development, mortality and other life history components. Where needed, Metabolic Theory could still reduce data requirements, but tactical models would ideally be parameterised with species-specific laboratory or field data. Such data could reveal additional covariates necessary to determine physiological rates, such as humidity or soil conditions (O'Connor *et al.* 2006), and it would be straightforward to include such predictors in our models. Additional species-specific life history details (e.g. time-/temperature-dependent egg production, hypobiosis, differing mortality rates between different developmental stages) may also be incorporated and could outline further sensitivities to climate. *Ostertagia gruehneri* egg production, for example, is seasonal, peaking in summer and dropping dramatically in fall (Stien *et al.* 2002), and this could interplay with climate warming-induced increases in summer mortality (Fig. 4) to disproportionately affect the species' ability to persist in future environments. Similarly, tactical models may include biological details to evaluate indirect climate change impacts, for instance, through changes in biodiversity, host range, or host immunity (Thieltges *et al.* 2008; Dobson 2009; Altizer *et al.* 2011). For instance, in the *O. gruehneri*-caribou system, phenological mismatches may arise between parasite and host availability due to seasonal changes in parasite viability (Fig. 4) and changes to host migration (Sharma *et al.* 2009). Ultimately, model complexity will depend on data availability and the model objectives, and may be determined using model selection tools (Burnham & Anderson 2002).

A recent review by Rohr *et al.* (2011) highlights three key, unresolved, questions to understanding climate change impacts on host–parasite systems. It remains unclear (1) at which geographical locations climate change will have the greatest impact, (2) which host–parasite systems might be most sensitive to climate change and (3) theory is needed that allows predicting the outcome of specific host–parasite interactions as a function of climate. The presented approach provides opportunities to address each of these questions, and thus a potential means for understanding and predicting climate change impacts on host–parasite systems worldwide. Metabolic models could, for example, generate R_0-maps for current and predicted climate scenarios as discussed above, thus quantifying the potential of given parasite species to establish and/or persist in certain regions. Such maps would be similar to maps arising from approaches like 'climate envelope modelling' (Pearson & Dawson 2003) – though potentially more informative due to their mechanistic underpinning (Mangal *et al.* 2008; Kearney & Porter 2009; Buckley *et al.* 2010) – and could outline likely areas of high impact. Traditionally, climate change is assumed to affect temperate and polar systems more than tropical ones due to the larger temperature increase at high latitudes (Dobson *et al.* 2008). However, some studies contend that tropical systems might be affected equally or more due to the narrower temperature tolerance of tropical ectotherms (Deutsch *et al.* 2008) or the larger absolute shift in metabolism for temperature changes at high relative to low baseline temperatures (Dillon *et al.* 2010). Although both these effects are easily quantified within our models, the predicted $R_0(T)$, and thus climate change impacts, will significantly depend on the model parameters, and particularly the activation energies (Fig. 3). These and other parameters, such as T^L and T^H, might systematically vary with latitude and other covariates (Clarke 2003; Irlich *et al.* 2009; Sunday *et al.* 2011), further emphasising the necessity to determine them for a broad range of parasites.

Similarly, our approach can be extended to other host–parasite systems, offering novel opportunities to assess which systems might be most sensitive to climate change. With ectotherm hosts, for example, temperature would not only affect the development and mortality of free-living stages but also host movement and parasite uptake rate, as well as the development, mortality and fecundity of hosts and parasites within hosts. Although these complexities may alter shape, magnitude and seasonality of R_0, the temperature-dependencies of all parameters may still be determined using Metabolic Theory (Brown *et al.* 2004; Dell *et al.* 2011). Extending these arguments further to different parasite groups, such as vector-transmitted parasites or parasites utilising intermediate hosts, could for example help addressing whether parasites with a direct or indirect life cycle are more sensitive to climate change (Rohr *et al.* 2011).

Finally, while our analyses have focused on parasite fitness and implications for parasite establishment and persistence, Metabolic Theory can be applied in similar ways to assess climatic impacts on other characteristics of host–parasite systems, such as transient dynamics, the stability of stationary states or the average parasite burden and prevalence in a host population (e.g. with burden, m, and prevalence, q, given by $m(T) = \lambda D_P \alpha_H{}^{-1} k_{NB}{}^{-1} \cdot (R_0(T)/C - 1/C)$ and $q(T) = 1 - (1 + m(T)/k_{NB})^{-k_{NB}}$ in a non-seasonal environment, Mangal *et al.* 2008). However, such analyses may depend substantially on model parameters other than those quantified here (e.g. the aggregation parameter k_{NB}; Grenfell *et al.* 1987), and may further

© 2012 Blackwell Publishing Ltd/CNRS

be affected in complex ways by parameters determining the timing of reproduction when seasonality is incorporated (e.g., the maturation delay τ_P or the presence/absence of hypobiosis), so we defer these assessments to future work.

Beyond host–parasite systems, the framework remains applicable because R_0 can be considered a measure of fitness in any species (de-Camino-Beck & Lewis 2008). With appropriate modification of eqns 1 and/or 7–9, our methods could thus complement non-seasonal metabolic population models that were developed for non-parasitic species and use alternate measures of fitness, such as the intrinsic growth rate, r_m (Amarasekare & Savage 2012). In sum, the generality of the approach suggests applications in a much broader context than examined here, for instance, for evaluating and/or predicting climate change impacts on the conservation of endangered species (Wikelski & Cooke 2006), or for proactively designing management strategies for expected, climate change-mediated, biological invasions (Walther *et al.* 2009).

AUTHORSHIP

PM, AD and SK jointly conceived the study. PM and AD developed and analysed the models. BH and SK collected the *O. gruehneri* data, which were analysed by PM, BH and SK. PM wrote the first draft of the manuscript, and all authors contributed substantially to revisions.

ACKNOWLEDGEMENTS

We are grateful to the James S. McDonnell Foundation, NSERC, and Alberta Innovates for funding this research.

REFERENCES

Allen, A.P., Gillooly, J.F. & Brown, J.H. (2005). Linking the global carbon cycle to individual metabolism. *Funct. Ecol.*, 19, 202–213.

Altizer, S., Bartel, R. & Han, B.A. (2011). Animal migration and infectious disease risk. *Science*, 331, 296–302.

Amarasekare, P. & Savage, V. (2012). A framework for elucidating the temperature dependence of fitness. *Am. Nat.*, 179, 178–191.

Anderson, R.M. & May, R.M. (1978). Regulation and stability of host-parasite population interactions: I. Regulatory processes. *J. Anim. Ecol.*, 47, 219–247.

Anderson, R.M. & May, R.M. (1991). *Infectious Diseases of Humans. Dynamics and Control*. Oxford University Press, New York, NY, p. 757.

Bolzoni, L., Dobson, A.P., Gatto, M. & De Leo, G.A. (2008). Allometric scaling and seasonality in the epidemics of wildlife diseases. *Am. Nat.*, 172, 818–828.

Brown, J.H., Gillooly, J.F., Allen, A.P., Savage, V.M. & West, G.B. (2004). Toward a metabolic theory of ecology. *Ecology*, 85, 1771–1789.

Buckley, L.B., Urban, M.C., Angiletta, M.J., Crozier, L.G., Rissler, L.J. & Sears, M.W. (2010). Can mechanism inform species' distribution models? *Ecol. Lett.*, 13, 1041–1054.

Burnham, K.P. & Anderson, D.R. (2002). *Model Selection and Multimodel Inference: A Practical Information-Theoretic Approach*. 2nd edn. Springer, New York, NY, p. 488.

Cable, J.M., Enquist, B.J. & Moses, M.E. (2007). The allometry of host-pathogen interactions. *PLoS ONE*, 2, e1130. doi: 10.1371/journal.pone.0001130.

de-Camino-Beck, T. & Lewis, M.A. (2008). On net reproductive rate and the timing of reproductive output. *Am. Nat.*, 172, 128–139.

Caswell, H. (2011). Beyond R_0: demographic models for variability of lifetime reproductive output. *PLoS ONE*, 6, e20809. doi:10.1371/journal.pone.0020809.

Clarke, A. (2003). Costs and consequences of evolutionary temperature adaptation. *Trends Ecol. Evol.*, 18, 573–581.

Dell, A.I., Pawar, S. & Savage, V.M. (2011). Systematic variation in the temperature dependence of physiological and ecological traits. *Proc. Nat. Acad. Sci.*, 108, 10591–10596.

Deutsch, C.A., Tewksbury, J.J., Huey, R.B., Sheldon, K.S., Ghalambor, C.K., Haak, D.C. *et al.* (2008). Impacts of climate warming on terrestrial ectotherms across latitude. *Proc. Nat. Acad. Sci.*, 105, 6668–6672.

Dillon, M.E., Wang, G. & Huey, R.B. (2010). Global metabolic impacts of recent climate warming. *Nature*, 467, 704–707.

Dixon, A.F.G., Honěk, A., Keil, P., Kotela, M.A.A., Šizling, A.L. & Jarošik, V. (2009). Relationship between the minimum and maximum temperature thresholds for development in insects. *Funct. Ecol.*, 23, 257–264.

Dobson, A. (2009). Climate variability, global change, immunity, and the dynamics of infectious diseases. *Ecology*, 90, 920–927.

Dobson, A.P. & Carper, R. (1992). Global warming and potential changes in host-parasite and disease-vector relationships. In: *Consequences of Global Warming for Biodiversity* (eds Peters, R.L. & Lovejoy, T.E.). Yale University Press, New Haven, CT, pp. 201–217.

Dobson, A.P. & Hudson, P.J. (1992). Regulation and stability of a free-living host-parasite system: *Trichostrongylus tenuis* in red grouse. II. Population models. *J. Anim. Ecol.*, 61, 487–498.

Dobson, A., Lafferty, K.D., Kuris, A.M., Hechinger, R.F. & Jetz, W. (2008). Homage to Linnaeus: how many parasites? How many hosts? *Proc. Nat. Acad. Sci.*, 105, 11482–11489.

Downs, C.J., Hayes, J.P. & Tracy, C.R. (2008). Scaling metabolic rate with body mass and inverse body temperature: a test of the Arrhenius fractal supply model. *Funct. Ecol.*, 22, 239–244.

Gillooly, J.F., Brown, J.H., West, G.B., Savage, V.M. & Charnov, E.L. (2001). Effects of size and temperature on metabolic rate. *Science*, 293, 2248–2251.

Grenfell, B.T., Smith, G. & Anderson, R.M. (1986). Maximum-likelihood estimates of the mortality and migration rates of the infective larvae of *Ostertagia ostertagi* and *Cooperia oncophora*. *Parasitology*, 92, 643–652.

Grenfell, B.T., Smith, G. & Anderson, R.M. (1987). A mathematical model of the population biology of *Ostertagia ostertagi* in calves and yearlings. *Parasitology*, 95, 389–406.

Györi, I. & Eller, J. (1981). Compartmental systems with pipes. *Math. Biosci.*, 53, 223–247.

Harvell, C.D., Mitchell, C.E., Ward, J.R., Altizer, S., Dobson, A.P., Ostfeld, R.S. *et al.* (2002). Climate warming and disease risks for terrestrial and marine biota. *Science*, 296, 2158–2162.

van der Have, T.M. (2002). A proximate model for thermal tolerance in ectotherms. *Oikos*, 98, 141–155.

Hechinger, R.F., Lafferty, K.D., Dobson, A.P., Brown, J.H. & Kuris, A.M. (2011). A common scaling rule for abundance, energetics, and production of parasitic and free-living species. *Science*, 333, 445–448.

Heesterbeek, J.A.P. & Roberts, M.G. (1995). Threshold quantities for helminth infections. *J. Math. Biol.*, 33, 415–434.

Hoar, B.M., Ruckstuhl, K. & Kutz, S. (2012). Development and availability of the free-living stages of *Ostertagia gruehneri*, an abomasal parasite of barrenground caribou (*Rangifer tarandus groenlandicus*), on the Canadian tundra. *Parasitology*, 139, 1093–1100.

Hoberg, E.P., Polley, L., Jenkins, E.J., Kutz, S.J., Veitch, A.M. & Elkin, B.T. (2008). Integrated approaches and empirical models for investigation of parasitic diseases in northern wildlife. *Emerg. Infect. Dis.*, 14, 10–17.

Huey, R.B., Deutsch, C.A., Tewksbury, J.J., Vitt, L.J., Hertz, P.E., Álvarez Pérez, H. *et al.* (2009). Why tropical forest lizards are vulnerable to climate warming. *Proc. R. Soc. B*, 276, 1939–1948.

IPCC (2007). *Climate Change 2007: The Physical Science Basis. Contribution of Working Group I to the Fourth Assessment Report of the Intergovernmental Panel on Climate Change*. Cambridge University Press, Cambridge, p. 996.

Irlich, U.M., Terblanche, J.S., Blackburn, T.M. & Chown, S.L. (2009). Insect rate-temperature relationships: environmental variation and the Metabolic Theory of Ecology. *Am. Nat.*, 174, 819–835.

Johnson, F.H. & Lewin, I. (1946). The growth rate of E. coli in relation to temperature, quinine and coenzyme. *J. Cell. Physiol.*, 28, 47–75.

de Jong, G. & van der Have, T.M. (2008). Temperature dependence of development rate, growth rate and size: from biophysics to adaptation. In: *Phenotypic Plasticity of Insects: Mechanisms and Consequences* (eds Whitman, D.W. & Ananthakrishnan, T.N.). Science, Enfield, pp. 461–526.

Kearney, M. & Porter, W. (2009). Mechanistic niche modeling: combining physiological and spatial data to predict species' ranges. *Ecol. Lett.*, 12, 334–350.

© 2012 Blackwell Publishing Ltd/CNRS

Kearney, M., Simpson, S.J., Raubenheimer, D. & Helmuth, B. (2010). Modelling the ecological niche from functional traits. *Phil. Trans. R. Soc. B*, 365, 3469–3483.

Kooijman, S.A.L.M. (2010). *Dynamic Energy Budget Theory for Metabolic Organisation*. 3rd edn. Cambridge University Press, Cambridge, p. 532.

Kutz, S.J., Hoberg, E.P. & Polley, L. (2001). *Umingmakstrongylus pallikuukensis* (nematoda: protostrongylidae) in gastropods: larval morphology, morphometrics, and development rates. *J. Parasitol.*, 87, 527–535.

Kutz, S.J., Hoberg, E.P., Polley, L. & Jenkins, E.J. (2005). Global warming is changing the dynamics of Arctic host-parasite systems. *Proc. R. Soc. B*, 272, 2571–2576.

Kutz, S.J., Jenkins, E.J., Veitch, A.M., Ducrocq, J., Polley, L., Elkin, B. *et al.* (2009). The Arctic as a model for anticipating, preventing, and mitigating climate change impacts on host-parasite interactions. *Vet. Parasitol.*, 163, 217–228.

Kutz, S.J., Ducrocq, J., Verocai, G.G., Hoar, B.M., Colwell, D.D., Beckman, K. B. *et al.* (2012). Parasites in ungulates of arctic North America and Greenland: a view of contemporary diversity, ecology, and impact in a world under change. *Adv. Parasitol.*, 79, 99–252.

Lafferty, K.D. (2009). The ecology of climate change and infectious diseases. *Ecology*, 90, 888–900.

de Leo, G.A. & Dobson, A.P. (1996). Allometry and simple epidemic models for microparasites. *Nature*, 379, 720–722.

Mangal, T.D., Paterson, P. & Fenton, A. (2008). Predicting the impact of long-term temperature changes on the epidemiology and control of schistosomiasis: a mechanistic model. *PLoS ONE*, 3, e1438. doi: 10.1371/journal.pone.0001438.

Marcogliese, D.J. (2001). Implications of climate change for parasitism of animals in the aquatic environment. *Can. J. Zool.*, 79, 1331–1352.

May, R.M. (1973). *Stability and Complexity in Model Ecosystems*. Princeton University Press, Princeton, NJ, p. 235.

May, R.M. & Anderson, R.M. (1979). Population biology of infectious diseases: part II. *Nature*, 280, 455–461.

McCauley, E., Nisbet, R.M., de Roos, A.M., Murdoch, W.W. & Gurney, W.S.C. (1996). Structured population models of herbivorous zooplankton. *Ecol. Monogr.*, 66, 479–501.

McCoy, M.W. & Gillooly, J.F. (2008). Predicting natural mortality rates of plants and animals. *Ecol. Lett.*, 11, 710–716. (Corrigendum. *Ecol. Lett.*, 12, 731-733).

Molnár, P.K., Derocher, A.E., Thiemann, G.W. & Lewis, M.A. (2010). Predicting survival, reproduction and abundance of polar bears under climate change. *Biol. Conserv.*, 143, 1612–1622.

Munch, S.B. & Salinas, S. (2009). Latitudinal variation in lifespan within species is explained by the metabolic theory of ecology. *Proc. Nat. Acad. Sci.*, 106, 13860–13864.

Nisbet, R.M., Muller, E.B., Lika, K. & Kooijman, S.A.L.M. (2000). From molecules to ecosystems through dynamic energy budget models. *J. Anim. Ecol.*, 69, 913–926.

O'Connor, L.J., Walkden-Brown, S.W. & Kahn, L.P. (2006). Ecology of the free-living stages of major trichostrongylid parasites of sheep. *Vet. Parasitol.*, 142, 1–15.

O'Connor, M.I., Gilbert, B. & Brown, C.J. (2011). Theoretical predictions for how temperature affects the dynamics of interacting herbivores and plants. *Am. Nat.*, 178, 626–638.

Pearson, R.G. & Dawson, T.P. (2003). Predicting the impacts of climate change on the distribution of species: are bioclimate envelope models useful? *Glob. Ecol. Biogeogr.*, 12, 361–371.

Pietrock, M. & Marcogliese, D.J. (2003). Free-living endohelminth stages: at the mercy of environmental conditions. *Trends Parasitol.*, 19, 293–299.

Poulin, R. (2006). Global warming and temperature-mediated increases in cercarial emergence in trematode parasites. *Parasitology*, 132, 143–151.

Régnière, J., Powell, J., Bentz, B. & Nealis, V. (2012). Effects of temperature on development, survival and reproduction of insects: experimental design, data analysis and modeling. *J. Insect Physiol.*, 58, 634–647.

Rogers, D.J. & Randolph, S.E. (2006). Climate change and vector-borne diseases. *Adv. Parasitol.*, 62, 345–381.

Rohr, J.R., Dobson, A.P., Johnson, P.T.J., Kilpatrick, A.M., Paull, S.H., Raffel, T. R. *et al.* (2011). Frontiers in climate change-disease research. *Trends Ecol. Evol.*, 26, 270–277.

Savage, V.M. (2004). Improved approximations to scaling relationships for species, populations, and ecosystems across latitudinal and elevational gradients. *J. Theor. Biol.*, 227, 525–534.

Schoolfield, R.M., Sharpe, P.J.H. & Magnuson, C.E. (1981). Non-linear regression of biological temperature-dependent rate models based on absolute reaction-rate theory. *J. Theor. Biol.*, 88, 719–731.

Sharma, S., Couturier, S. & Côté, S.D. (2009). Impacts of climate change on the seasonal distribution of migratory caribou. *Global Change Biol.*, 15, 2549–2562.

Sharpe, P.J.H. & DeMichele, D.W. (1977). Reaction kinetics of poikilotherm development. *J. Theor. Biol.*, 64, 649–670.

Smith, G. (1990). The population biology of the free-living phase of *Haemonchus contortus*. *Parasitology*, 101, 309–316.

Smith, G., Grenfell, B.T. & Anderson, R.M. (1986). The development and mortality of the non-infective free-living stages of *Ostertagia ostertagi* in the field and in laboratory culture. *Parasitology*, 92, 471–482.

Stien, A., Irvine, R.J., Langvatn, R., Albon, S.D. & Halvorsen, O. (2002). The population dynamics of *Ostertagia gruehneri* in reindeer: a model for the seasonal and intensity dependent variation in nematode fecundity. *Int. J. Parasitol.*, 32, 991–996.

Sunday, J.M., Bates, A.E. & Dulvy, N.K. (2011). Global analysis of thermal tolerance and latitude in ectotherms. *Proc. R. Soc. B*, 278, 1823–1830.

Thieltges, D.W., Jensen, K.T. & Poulin, R. (2008). The role of biotic factors in the transmission of free-living endohelminth stages. *Parasitology*, 135, 407–426.

Trudgill, D.L., Honek, A., Li, D. & van Straalen, N.M. (2005). Thermal time – concepts and utility. *Ann. Appl. Biol.*, 146, 1–14.

Vasseur, D.A. & McCann, K.S. (2005). A mechanistic approach for modeling temperature-dependent consumer-resource dynamics. *Am. Nat.*, 166, 184–198.

Walther, G.R., Roques, A., Hulme, P.E., Sykes, M.T., Pyšek, P., Kühn, I. *et al.* (2009). Alien species in a warmer world: risks and opportunities. *Trends Ecol. Evol.*, 24, 686–693.

Wikelski, M. & Cooke, S.J. (2006). Conservation physiology. *Trends Ecol. Evol.*, 21, 38–46.

Young, R.R., Nicholson, R.M., Tweedie, R.L. & Schuh, H.J. (1980). Quantitative modelling and prediction of development times of the free-living stages of *Ostertagia ostertagi* under controlled and field conditions. *Parasitology*, 81, 493–505.

SUPPORTING INFORMATION

Additional Supporting Information may be downloaded via the online version of this article at Wiley Online Library (www.ecologyletters.com).

Editor, Michael Bonsall
Manuscript received 14 June 2012
First decision made 23 July 2012
Second decision made 13 September 2012
Manuscript accepted 24 September 2012

© 2012 Blackwell Publishing Ltd/CNRS